

# A Quotient Space Formulation for Statistical Analysis of Graphical Data

Xiaoyang Guo, Anuj Srivastava, *Fellow, IEEE* and Sudeep Sarkar, *Fellow, IEEE*

**Abstract**—Complex analyses involving multiple, dependent random quantities often lead to graphical models – a set of nodes denoting variables of interest, and corresponding edges denoting statistical interactions between nodes. To develop statistical analyses for graphical data, one needs mathematical representations and metrics for matching and comparing graphs, and other geometrical tools, such as geodesics, means, and covariances, on representation spaces of graphs. This paper utilizes a quotient structure to develop efficient algorithms for computing these quantities, leading to useful statistical tools, including principal component analysis, linear dimension reduction, and analytical statistical modeling. The efficacy of this framework is demonstrated using datasets taken from several problem areas, including alphabets, video summaries, social networks, and biochemical structures.

**Index Terms**—Graph summaries, modeling graph variability, graph matching, graph PCA.

## I. INTRODUCTION

**D**UE to rapid advances in sensing and measurement technology, data is increasingly becoming complex and structured, reflecting the growing needs for newer approaches and problem formulations. One common approach to understanding complex, high-dimensional datasets is to represent them as graphs. Typically one identifies a number of variables of interests in the data, designating them as nodes, and represents their interactions as edges in a graph. Such a graph captures variability and interactions associated with a large number of variables, and is amenable to higher-order statistical analysis. Examples of graphical representations can be found in many areas, including video data analysis [1], social networks [2], gene expression networks [3], brain connectivity data [4], geographical data [5], financial stocks [6], communication networks [7], epidemiology [8], and so on. Fig. 1 shows some examples: letters with straight edges, molecules with atoms as nodes and valence as edges, videos represented as pattern theoretic graphs [1] with objects or actions as nodes and their relationships as edges, and brain connectivity networks in Human Connectome Project (HCP) [9] data.

The use of graph representations is of great interest in machine learning, including deep learning. In principle all geometric deep learning is concerned with learning on *manifold of the data elements (nodes)* which, in turn, can be naturally represented by a graph. Additionally, there are

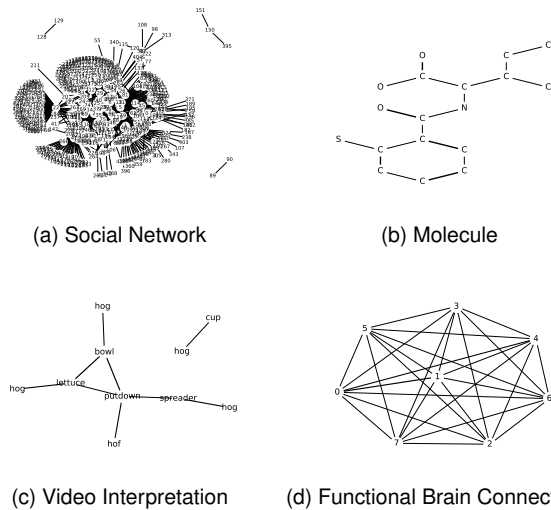


Fig. 1. Some examples of graphs representing knowledge in different applications.

some papers that consider entire graphs as the entities of interest. For instance, papers, such as `graph2vec` [10] and `UgraphEmbed` [11], consider the problem of assigning a fixed vector space representation to entire graphs. Some other papers seek to find vector representations for nodes such that distances in the vector space is reflective of the neighborhood structure of the graph. Examples include modeling random-walks through the nodes using recursive neural networks (RNN) [12], [13], or ones that preserves first and second-order proximity information [14], [15], or ones that consider larger neighborhood structures as captured by node coarsening [16]. Another set of papers seek to perform graph convolutions, i.e. convolutions over the nodes, respecting the manifold defined by the given graph. Examples include graph signal processing [17], [18], or works that direct processing via the local graph structure [19], [20]. Again, like the previous embedding problem this one too considers a single graph and operations on the nodes of that graph.

We are focused on the problems where one has several graphs, each representing a snapshot or an observation of a system at any instance, and one is interested in capturing, modeling and analyzing *statistical variability across these graphs*. For instant, consider the representation of functional connectivity of parts of a human brain during performance of a certain task, as measured by fMRI signals, using graphical structures. Given several such graphs, one for each human subject under each task and performance, one has a large

X. Guo, A. Srivastava are with the Department of Statistics, Florida State University, Tallahassee, FL 32306, USA. e-mail: {xiaoyang.guo, anuj}@stat.fsu.edu

S. Sarkar is with Department of Computer Science and Engineering, University of South Florida, Tampa, FL 33620, USA. e-mail: sarkar@usf.edu

Manuscript received April 19, 2005; revised August 26, 2015.

amount of graph data to analyze and model. Similarly, one may have graphical representations of different social or economic networks, each representing different communities. The general goal of statistical analysis is: (1) derive *common characteristics across observed graphs*, (2) *distinguish graph populations* using statistical testing, and (3) model variability in graph data using *analytical generative models*. Thus, a unique aspect of this work is that we can create a generative model over entire graphs. We can generate synthetic graphs that capture dominant variability of the domain. An interesting short-term use of the generative aspects can be to augment training data for other graph-based deep learning approaches. In the long term, our hope is that the theory in this paper will enable the study of deep learning on *non-Euclidean manifolds of graphs*, where the data elements are themselves graphs.

The structured nature of graphs makes them difficult to analyze using classical statistical tools. A graph is a non-Euclidean data object that consists of a set of variables in form of nodes and their interactions in form of edges. There are two sources of variability in graphs – (i) different number and values (attributes) of nodes, and (ii) different connectivity patterns of the nodes (in form of edges). One is interested in incorporating both these factors in comparisons and analyses of graphs. Learning structures underlying observed graphs can help us understand deeper relationships between the variables of interests. Therefore, one is interested in mathematical representations that enable quantitative statistical analysis of graph data in terms of both edge and node attributes. For quantifying differences across graphs, one requires metrics that can incorporate an arbitrary combination of differences in these properties. However, one big issue in analyzing graph data is that nodes across graphs often come without matchings or correspondences. The problem of establishing correspondences of nodes across graphs is called *registration (or graph matching)* and it represents one of the biggest challenges in statistical analysis of graphs.

In the literature, there are mainly two different types of graph matching: exact matching and inexact matching [21]. The exact matching implies finding a bijective map such that the nodes and edges across two graphs are in one-to-one correspondence. If two graphs can be matched exactly, then the mapping is also called an *isomorphism*. A related topic is *subgraph isomorphism* [22] where one graph matches to a substructure of another graph. In contrast, the inexact matching seeks optimal registration between graphs that may be dissimilar. The inexact matching is more common in practice because of the complexities associated with real data. Since matching of two sets of nodes is essentially a problem of combinatorics, the problem of finding a global optimum for inexact graph matching is NP hard [23]. Therefore, most algorithms for graph matching seek approximate solutions based on different relaxations of the original problem [24]. As described later, the mathematical variability of matching different nodes across graphs is achieved using the action of a permutation group – a permutation of ordering of nodes in graph changes its registration with an ordered set of nodes representing another graph. The approximate solutions correspond to expanding from the permutation group to some larger set where the

solutions are more readily available. One idea is to replace permutations by rotation matrices and then use spectral (eigen-decomposition based) approaches to find optimal rotations, see [25], [26]. Another direction is to replace permutations by doubly stochastic matrices, and find the solution in that larger space. In all these cases, the final solution can eventually be restricted to the discrete set of permutation matrices, see e.g. [27], [28]. Besides these approximations, there are some other algorithms for approximate graph matching [29]–[31]. There are also some tree-search based methods to calculate the graph edit distance (GED) [21], a problem that incorporates graph matching. The general idea here is to solve the problem iteratively – given the current estimation of cost (based on pre-defined cost of node/edge insertion, deletion and substitution), determine the next operation based on the heuristic estimation of future cost, see [32].

In this paper we present a metric-based approach for comparing, summarizing, and analyzing graphs. The basic idea is to represent graphs as matrices, and to formulate the registration problem as that of permutation of entries in those matrices. Mathematically speaking, we represent the registration variability using the action of the permutation group on the set of matrices representing all graphs. In order to remove this nuisance group, we form a quotient space and inherit a metric on the quotient space from the original set of matrices. We use a standard Euclidean metric, with appropriate invariance properties, because it allows for an efficient registration of nodes across graphs. The quotient space metric is then used to define and compute statistical summaries such as clustering, sample means, covariances, and principal components. The principle component analysis can be used to perform dimension reduction, and to impose compact statistical models on observed graphs. These models can play important roles in hypothesis testing and other statistical inferences involving graph data.

The novel contributions of this paper are as follows:

- 1) It adapts a quotient space metric structure on the set of graph representations, originally introduced in [33], and extends it to include both node and edge attributes. It uses this metric structure to quantify graph differences and to compute optimal deformations (geodesics) between graphs. Using this metric structure, it establishes a framework for computing sample statistics such as mean and covariance for graph data.
- 2) A key idea here is that it does not assume the graphs to be isomorphic. That is, one allows nodes to remain unmatched across the graphs. Past metric-based approaches often insist on every node being matched to a proper node during graph comparisons.
- 3) It defines the notion of principal component analysis of graphs, and uses that to develop low-dimensional representations of observed graphs.
- 4) It develops a simple Gaussian-type model for capturing graph variability in observed graphs and uses it to generate random samples from such graphical models. This sampling, in turn, can be used for Bayesian inferences involving graphical data although that direction has not been pursued here.

The rest of this paper is organized as follows. Section II describes the chosen mathematical representation of graphs using symmetric matrices. Section III studies the graph matching problem using an action of the permutation group. Section IV extends this framework to include both node and edge attributes in the framework. Section V presents techniques for statistical analysis of graph data. Section VI shows a number of experiments illustrating this framework. The paper ends with a short discussion and some conclusions in Section VII.

## II. GRAPH REPRESENTATION AND METRIC STRUCTURE

In this section, we will present a framework for the structure of graphs that was first developed in [33], [34]. We apply and advance this framework as described below.

### A. Adjacency Matrix Representation

We start by providing a mathematical representation for analyzing weighted graphs. A weighted graph  $G$  is an ordered pair  $(V, w)$ , where  $V$  is a set of nodes and  $w$  is a weighting function:  $w : V \times V \rightarrow M$ .  $M$  is a Riemannian manifold on which we can define distances, averages, and covariances. That is,  $w(v_i, v_j)$  characterizes the edge between  $v_i, v_j \in V, i \neq j$ , where elements of the set  $E = \{(v_i, v_j) \in V \times V : i \neq j\}$  are the edges of  $G$ . A binary graphs is the special case of weighted graphs where the weights of edges are either zero or one. Assuming that the number of nodes, denoted by  $|V|$ , is  $n$ ,  $G$  can be represented by its adjacency matrix  $A = \{a_{ij}\} \in M^{n \times n}$ , where the element  $a_{ij} = w(v_i, v_j)$ . For an undirected graph  $G$ , we have  $w(v_i, v_j) = w(v_j, v_i)$  and therefore  $A$  is a symmetric matrix. (In this paper, we only focus on undirected graphs although the framework is extendable to directed graphs also.) The set of all such matrices is given by  $\mathcal{A} = \{A \in M^{n \times n} | A = A^T, \text{diag}(A) = 0\}$ . Let  $d_m$  denote the Riemannian distance on  $M$ . We will use this to impose a metric on the representation space  $\mathcal{A}$ . That is, for any two  $A_1, A_2 \in \mathcal{A}$ , with the corresponding entries  $a_{ij}^1$  and  $a_{ij}^2$ , respectively, the metric  $d_a(A_1, A_2) \equiv \sqrt{\sum_{i,j} d_m(a_{ij}^1, a_{ij}^2)^2}$  quantifies the difference the graphs they represent. Under the chosen metric, the geodesic or the shortest path between two points in  $\mathcal{A}$  can be written as a set of geodesics in  $M$  between the corresponding components. That is, for any  $A_1, A_2 \in \mathcal{A}$ , the geodesic  $\alpha : [0, 1] \rightarrow \mathcal{A}$  consists of components  $\alpha = \{\alpha_{ij}\}$  given by  $\alpha_{ij} : [0, 1] \rightarrow M$ , a geodesic path in  $M$  between  $a_{ij}^1$  and  $a_{ij}^2$ . In case  $M = \mathbb{R}$ , then  $\mathcal{A}$  is a vector space, equivalent to a Euclidean space of dimension  $n(n+1)/2$ , and the geodesic between two points in  $\mathcal{A}$  is a straight line. That is, for any  $A_1, A_2 \in \mathcal{A}$ ,  $\alpha : [0, 1] \rightarrow \mathcal{A}$  given by  $\alpha(t) = (1-t)A_1 + tA_2$  is the geodesic path.

Since the ordering of nodes in graphs is often arbitrary, the ensuing analysis should not be dependent on this arbitrary choice. We view the ordering variability as a nuisance and seek to remove its influence from the analysis. A different way to state this issue is that nodes across graphs need to be registered during comparisons, and we will use permutations to perform registration. Let  $\mathcal{P}$  be the set of all permutation matrices of size  $n \times n$ . A permutation matrix is a matrix that has exactly

one 1 in each row and each column, with all the other entries being zero. This set forms a group with the group operation being matrix multiplication, and the identity element being the  $n \times n$  identity matrix. Note that  $\mathcal{P}$  is a subgroup of  $SO(n)$ , the set of all  $n \times n$  rotation matrices. For any  $P \in \mathcal{P}$ , the inverse of  $P$  is given by  $P^T$ , the transpose of  $P$ . We define the action of  $\mathcal{P}$  on  $\mathcal{A}$  using the map:

$$\mathcal{P} \times \mathcal{A} \mapsto \mathcal{A}, \quad (P, A) = PAP^T.$$

One can easily verify that this is a proper group action. For any  $A \in \mathcal{A}$ , its orbit under the action of  $\mathcal{P}$  is given by:

$$[A] = \{PAP^T | P \in \mathcal{P}\}.$$

It is the set of all possible permutations of the node ordering in a graph represented by  $A$ . Any two elements of an orbit denote exactly the same graph, except that the ordering of the nodes has been changed. Therefore, the membership of an orbit defines an equivalent relationship  $\sim$  on the set  $\mathcal{A}$ :

$$A_1 \sim A_2 \Leftrightarrow \exists P \in \mathcal{P} : PA_1P^T = A_2. \quad (1)$$

One can check that any two orbits  $[A_1]$  and  $[A_2]$ , for any  $A_1, A_2 \in \mathcal{A}$ , are either equal or disjoint. The set of all equivalence classes forms the quotient space or the *graph space*:

$$\mathcal{G} \equiv \mathcal{A}/\mathcal{P} = \{[A] | A \in \mathcal{A}\}. \quad (2)$$

$\mathcal{G}$  is a nonlinear space because it is a quotient space – one cannot perform linear operations, such as addition or multiplications on its elements directly. For example,  $x_1[A_1] + x_2[A_2]$  is not well defined in  $\mathcal{G}$  for arbitrary  $x_1, x_2 \in \mathbb{R}$ . Next we will impose a metric structure on this quotient space, and use this metric to compute statistical summaries and to perform statistical analysis.

We can inherit the chosen distance (the Frobenious norm) from  $\mathcal{A}$  on to the quotient space  $\mathcal{G}$  due to the following result.

*Lemma 1:* The action of  $\Gamma$  on  $\mathcal{A}$  is by isometries. That is, for any  $A_1, A_2 \in \mathcal{A}$  and  $P \in \mathcal{P}$ , we have

$$d_a(PA_1P^T, PA_2P^T) = d_a(A_1, A_2). \quad (3)$$

The proof is easy since an identical permutation on both graphs leaves the registration between nodes (across graphs) remains unchanged. Also, since  $\mathcal{P}$  is a finite set, the orbits under  $\mathcal{P}$  are finite. This enables the following definition.

*Definition 1 (Graph Metric):* Define a metric on the graph space  $\mathcal{G}$  according to:

$$\begin{aligned} d_g([A_1], [A_2]) &= \min_{P \in \mathcal{P}} d_a(A_1, PA_2P^T) \\ &= \min_{P \in \mathcal{P}} d_a(A_2, PA_1P^T) \end{aligned} \quad (4)$$

Since  $\mathcal{P}$  is a finite set, the minimum is well defined. The last equality comes from the fact that the action of  $\mathcal{P}$  is by isometry (Eqn. 3) and that  $\mathcal{P}$  is a group.

One can define geodesics in the graph space  $\mathcal{G}$  as follows. For any two graphs, with the adjacency matrices  $A_1$  and  $A_2$ , let  $P^*$  denote the optimal permutation of  $A_2$  to best register it with  $A_1$  (according to Eqn. 4). Then, the geodesic path between  $[A_1]$  and  $[A_2]$  in  $\mathcal{G}$  is given by the line  $t \mapsto [\alpha(t)]$ , where the components  $\alpha_{ij}(t)$  denote geodesics in  $M$  between

the registered elements of  $A_1$  and  $P^*A_2P^{*T}$ . This geodesic, in turn, is useful in computing graph summaries and graph PCA, as defined later.

### B. Alternative Representation: Laplacian Matrix

In the special case when  $M = \mathbb{R}$ , one can also use graph Laplacian matrix [35], [36] as a mathematical representation, instead of the adjacency matrix, for a graph. The graph Laplacian matrix  $L = [l_{ij}]$  is defined as follows:

$$l_{ij} = \begin{cases} -w(v_i, v_j), & \text{if } i \neq j \\ \sum_{k \neq i} w(v_i, v_k), & \text{if } i = j. \end{cases}$$

The set of all such Laplacian matrices is given by  $\mathcal{L}$ , the set of all positive semidefinite matrices of size  $n \times n$ . There is a bijective mapping between adjacency matrices and Laplacian matrices  $\phi : \mathcal{A} \rightarrow \mathcal{L}$  with  $\phi$  defined as follows. Suppose  $A$  is an adjacency matrix and  $L$  is the Laplacian matrix for the same graph  $G$ . Then,  $L = \phi(A) = D - A$ , where  $D = \text{diag}(A(\mathbf{1}\mathbf{1}^T - I))$  and  $\mathbf{1}$  is the vector of all ones. The inverse of  $\phi$  is given by:  $\phi^{-1} : \mathcal{L} \rightarrow \mathcal{A}$ ,  $A = \phi^{-1}(L) = \text{diag}(L) - L$ . The bijection of  $\phi$  can be proved as follows. First, if  $L_1 = L_2$ ,  $D_1 - A_1 = D_2 - A_2$  and it implies  $A_1 = A_2$  (Injection). And  $\forall L \in \mathcal{L}$ , we can find the pre-image  $A = \text{diag}(L) - L \in \mathcal{A}$  (Surjection). There are some interesting properties associated with the two representations:

- 1) Since  $\text{diag}(PAP^T(\mathbf{1}\mathbf{1}^T - I)) = P\text{diag}(A(\mathbf{1}\mathbf{1}^T - I))P^T$ , we have  $\phi(PAP^T) = P\phi(A)P^T$ , for all  $P \in \mathcal{P}$ .
- 2) For any geodesic path  $\alpha(t) = (1-t)A_1 + tA_2$  in  $\mathcal{A}$ , the corresponding path in  $\mathcal{L}$  is given by:  $\beta(t) = \phi(\alpha(t))$

$$\begin{aligned} &= (1-t)(\text{diag}(A_1(\mathbf{1}\mathbf{1}^T - I)) - A_1) + t(\text{diag}(A_2(\mathbf{1}\mathbf{1}^T - I)) - A_2) \\ &= \text{diag}(((1-t)A_1 + tA_2)(\mathbf{1}\mathbf{1}^T - I)) - ((1-t)A_1 + tA_2) \\ &= (1-t)L_1 + tL_2. \end{aligned}$$

Note that  $\beta(t)$  is generally not a geodesic path in  $\mathcal{L}$  under the commonly used metrics on  $\mathcal{L}$ .

- 3) Also, under the Frobenious norms on  $\mathcal{A}$  and  $\mathcal{L}$ , the mapping  $\phi$  is not isometric, i.e.  $\|\phi(A_1) - \phi(A_2)\| \neq \|A_1 - A_2\|$ , in general.

The framework developed in this paper can also be alternatively applied to the Laplacian representation, instead of the adjacency representation. For simplicity, we mainly focus on the latter in this paper.

### III. GRAPH MATCHING PROBLEM

The problem of optimizing over  $\mathcal{P}$ , as stated in Eqn. 4, becomes a key step in evaluating the graph metric and performing statistical analysis. Let  $G_1 = (V_1, w_1), G_2 = (V_2, w_2)$  be any two weighted graphs, and let  $A_1, A_2$  be the corresponding adjacency matrices. To simplify the discussion on graph matching and existing literature, we will completely focus on the case where  $M = \mathbb{R}$ . (The problem of matching nodes, when entries of  $A$  are elements of arbitrary nonlinear manifolds, remains unsolved.) Then, the registration requires solving the problem:

$$P^* = \underset{P \in \mathcal{P}}{\text{argmin}} \|PA_1P^T - A_2\|^2. \quad (5)$$

Most of current graph matching algorithms are applicable only to graphs with equal number of nodes. Even if they allow different number of nodes, they require that each node of the smaller graph must be registered to at least one node in the larger graph. Here 'smaller' and 'larger' indicate the size of the graphs, i.e. the number of nodes.

In general, given two graphs,  $G_1$  with  $n_1$  nodes and  $G_2$  with  $n_2$  nodes and  $n_1 \neq n_2$ , we will add  $n_2, n_1$  null nodes to  $G_1, G_2$ , respectively, to bring each of them to the same size  $n_1 + n_2$ . The null nodes are unattached nodes with zero values for the node attributes. As a result, the new adjacency matrices of  $G_1$  and  $G_2$  are:

$$A'_1 = \begin{pmatrix} A_1 & 0_{n_1 \times n_2} \\ 0_{n_2 \times n_1} & 0_{n_2 \times n_2} \end{pmatrix}, \quad A'_2 = \begin{pmatrix} A_2 & 0_{n_2 \times n_1} \\ 0_{n_1 \times n_2} & 0_{n_1 \times n_1} \end{pmatrix}. \quad (6)$$

The new matrix dimensions are  $A'_1, A'_2 \in \mathbb{R}^{(n_1+n_2) \times (n_1+n_2)}$  and, therefore, one can now apply previous graph matching algorithms. In fact, this idea of extending the adjacency matrix using Eqn. 6, can be applied even when the graphs being compared have same number of nodes, in order to allow for individual nodes to match with null nodes. By doing this, one has more degrees of freedom, in order to reach a better matching and to further reduce the cost function.

In the next three subsections, we present three different solutions for this optimization problem over  $\mathcal{P}$ .

#### A. Umeyama Algorithm

First we introduce a classic solution from [25] that is based on eigen decomposition of representation matrices. This method is summarized in Algorithm 1 and not repeated in the text here. Note that Algorithm 1 applies to the current discussion with  $\lambda = 0$ , the more general case is discussed later in Section IV. As noted in [25], the solution  $P$  is the global solution for isomorphic graphs but is usually a good initialization to more general graph matching problems. Thus, we use it as an initial condition for a greedy search (pairwise exchanges of rows and columns) that seeks to further improve the solutions.

We illustrate this idea using some simple examples in Fig. 2. This dataset has binary graphs representing uppercase English letters [37]. Each row shows the original graphs  $G_1$  (first graph) and  $G_2$  (last graph), and the outcomes  $G_{1p}$  and  $G_{2p}$ , in the middle.  $G_{1p}$  is the optimal permutation from Algorithm 1 of  $G_1$ , while  $G_{2p}$  is same as  $G_2$  with possibly some null nodes added. The first row shows the simpler case, where  $G_1$  and  $G_2$  have same number of nodes. We still add null nodes to both of them and permute  $G_1$  to match  $G_2$ , resulting in  $G_{1p}$ . As expected, the null nodes of  $G_1$  are found to be registered to null nodes of  $G_2$ , and are not displayed here. For the second row, the graphs  $G_1$  and  $G_2$  have different sizes. It is interesting to note that  $G_{2p}$  has a null node – node 5 – which means a regular node 5 of  $G_{1p}$  is registered to a null node of  $G_{2p}$ . In the last row, the two graphs  $G_1$  and  $G_2$  have the same size. However, both  $G_{1p}$  and  $G_{2p}$  have null nodes (2 and 5, respectively), that are matched to the regular nodes of the other graph. This seems to result in a more natural matching.

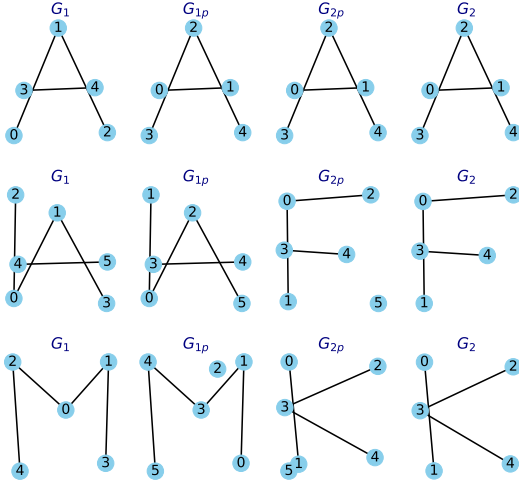


Fig. 2. Examples of graph matching using edge weights. In each row, the corner graphs, labeled  $G_1$  and  $G_2$ , are the original graphs. The inner two,  $G_{1p}$  and  $G_{2p}$ , are outcomes that are matched to each other. The outcome graphs may have some null nodes added, and the indices of  $G_1$  are permuted as  $G_{1p}$ .

### B. Fast Approximate Quadratic Programming

Algorithm 1 generally works well for smaller graphs but becomes slow when the number of nodes gets large. The greedy part of this algorithm costs  $\mathcal{O}(n^2)$  in computations for each node exchange. Recently, [28], [38] have used the Frank-Wolfe algorithm [39] to develop a different solution, called *Fast Approximate Quadratic* or FAQ. The main idea is to restate matching problem according to:

$$\min_{P \in \mathcal{P}} \|PA_1P^T - A_2\|^2 = \min_{P \in \mathcal{P}} (-\text{Tr}(A_2PA_1P^T)) .$$

The RHS of above equation is a special case of quadratic assignment problem. One can solve it using the gradient of the cost function  $f(P) = -\text{Tr}(A_2PA_1P^T)$ . In order to handle the discrete nature of permutation matrix, the procedure first replaces the permutation matrix by a doubly stochastic matrix:

$$\min_{P \in \mathcal{D}} f(P) = \min_{P \in \mathcal{D}} (-\text{Tr}(A_2PA_1P^T)) , \quad (7)$$

where  $\mathcal{D}$  is the set of doubly stochastic matrices. These are matrices whose: (1) all entries are non-negative, and (2) rows sum, columns sum equal to one. After the optimization, the solution  $P$  is projected back to the space  $\mathcal{P}$ . We summarize this approach in Algorithm 2, with the current context applicable for  $\lambda = 0$ .

### C. Comparisons of Algorithms for Registration

We compare these two algorithms, along with famous graduate assignment algorithm [27], using some simulated data. Algorithm 1 was run in Python 3.6.8 while FAQ and graduate assignment was run in Matlab, R2018b. All three were run on the same machine with a 2.5 GHz Intel Core i7 CPU. For each pair of graphs, we apply these three algorithms, and record the energy, i.e., the optimal cost ( $\|PA_1P^T - A_2\|^2$ ) and the elapsed time. For graduate assignment, the parameters

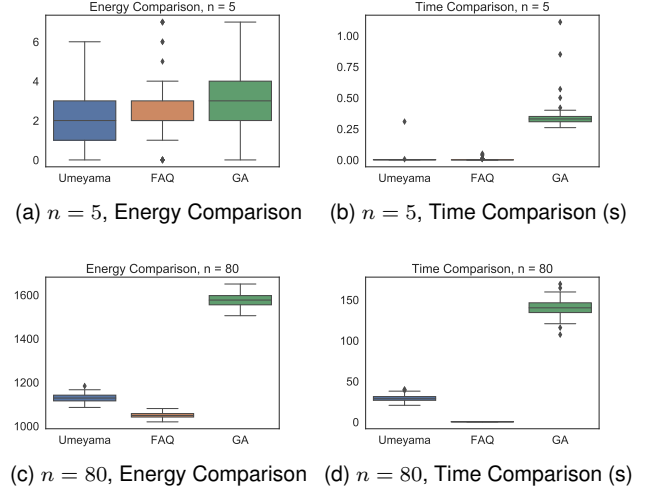


Fig. 3. Comparison between different graph matching algorithms.

used are  $\beta_0 = 0.05, \beta_f = 30, \beta_r = 1.05, I_0 = 20, I_1 = 200$ . We show the results in Fig. 3.

- 1) Case 1: We randomly generate 100 pairs of Erdős-Rényi graphs (binomial graphs) [40] with number of nodes  $n = 5$  and probability  $p = 0.5$  for edges.
- 2) Case 2: We repeat the same procedure for graphs with  $n = 80$  and  $p = 0.5$ .

As the first row shows, for smaller graphs ( $n = 5$ ), Algorithm 1 has better performance. For large graphs ( $n = 80$ ), FAQ is both superior in terms of both energy and time. These experiments tell us that different graph sizes demand different matching algorithms.

## IV. EXTENSION INVOLVING BOTH EDGE WEIGHTS AND NODE ATTRIBUTES

In many cases, the structure of a graph can be identified by comparing edge weight exclusively. However, sometimes the information associated with the nodes of graphs is also important in matching and comparing graphs. Next we extend the previous framework to incorporate node information also.

Let  $\mathcal{N}$  be the set of potential node attributes and let  $\epsilon \in \mathcal{N}$  be a distinguished element denoting the null or void element. A node-attributed weighted graph is represented by  $G = (V, w, \alpha)$ , consisting of: (i) a finite nonempty set  $V$  of nodes, (ii) a weight function  $w$  for edges, and (iii) an attribute function for nodes given by  $\alpha : V \rightarrow \mathcal{N}$ . Let  $d_\alpha$  be an appropriate distance in  $\mathcal{N}$ ,  $d_\alpha : \mathcal{N} \times \mathcal{N} \rightarrow \mathbb{R}^*$ .

For any two graphs  $G_1 = (V_1, w_1, \alpha_1)$  and  $G_2 = (V_2, w_2, \alpha_2)$ , each with  $n$  nodes, let  $D$  denote the  $n \times n$  matrix of pairwise distances between nodes across the two graphs. That is,  $D = [d_{ij} = d(\alpha(v_i), \alpha(v_j))^2] \in \mathbb{R}^{n \times n}$ , where  $v_i \in V_1, v_j \in V_2, i, j = 1, 2, \dots, n$ . Now the matching problem becomes:

$$P = \underset{P \in \mathcal{P}}{\text{argmin}} \{ \|PA_1P^T - A_2\|^2 + \lambda \text{Tr}(PD) \} , \quad (8)$$

where  $\lambda > 0$  is the tuning parameter to balance the contributions of edge and node attributes in matching. For FAQ, the equivalent matching problem is defined as:

$$P = \operatorname{argmin}_{P \in \mathcal{P}} [-\operatorname{Tr}(A_2 P A_1 P^T) + \lambda \operatorname{Tr}(P D)] . \quad (9)$$

The new gradient for Eqn. 9 becomes  $-A_2 P A_1^T - A_2^T P A_1 + \lambda D^T$ . The previous algorithms can be simply modified to handle the new formulation. In fact these general solutions are already presented in Algorithms 1 and 2 for a general  $\lambda$ .

More generally, for  $G_1, G_2$  with  $n_1, n_2$  ( $n_1 \leq n_2$ ) nodes, we extend the  $n_1 \times n_1$  matrix  $D$  according to:

$$D' = \begin{pmatrix} D & D_{n_1 \times n_2}^* \\ D_{n_2 \times n_1}^* & 0_{n_2 \times n_2} \end{pmatrix} . \quad (10)$$

Here, the off-diagonal elements  $d_{ij} = d(\alpha(v_i), \epsilon)^2$  in  $D_{n_1 \times n_2}^*$  represent the node-attribute distance between  $v_i \in V_1$  and  $j$ th null node  $\epsilon$  in  $G_2$ . The explanation applies to  $D_{n_2 \times n_1}^*$  as well.

---

### Algorithm 1 Umeyama with Extension Involving Node Attributes

---

Given graphs  $G_1$  and  $G_2$  and the associated adjacency matrices  $A_1$  and  $A_2$ , and  $D$  is the node attribute distance matrix.

- 1: Compute the eigendecompositions  $A_1 = U_1 \Sigma_1 U_1^T$  and  $A_2 = U_2 \Sigma_2 U_2^T$
  - 2: Find  $P = \operatorname{argmax} \operatorname{Tr}(P^T (\bar{U}_1 \bar{U}_2^T - \lambda D^T))$  using the Hungarian algorithm [41]. As earlier,  $\bar{U}_i, i = 1, 2$  denotes a matrix with values that are magnitudes of the corresponding elements of  $U_i$ .
  - 3: (Optional) Find the best exchange of two nodes of  $G_1$  based on  $P$ , call it  $P^*$ , such that  $P^* = \operatorname{argmin} \|P A_1 P^T - A_2\|^2 + \lambda \operatorname{Tr}(P D)$  and update  $P = P^*$
  - 4: Repeat 3 until the value of  $\|P A_1 P^T - A_2\|^2 + \lambda \operatorname{Tr}(P D)$  does not decrease.
- 

---

### Algorithm 2 FAQ with Extension Involving Node Attributes

---

Given graphs  $G_1$  and  $G_2$  and the associated adjacency matrices  $A_1$  and  $A_2$ .

- 1: Choose an initial  $P \in \mathcal{P}$ .
  - 2: Compute the gradient of  $f(P)$ :  $\nabla f(P) = -A_2 P A_1^T - A_2^T P A_1 + \lambda D^T$ .
  - 3: Approximate  $f(P)$  by first order Taylor expansion around the current estimate  $P^*$ :  $f(P) \approx f(P^*) + \nabla f(P^*)^T (P - P^*)$  and use Hungarian algorithm to minimize it, get  $Q$ .
  - 4: Line search to determine the optimal step size  $\alpha \in (0, 1)$
  - 5: Update the doubly stochastic matrix  $P^* = P^* + \alpha(Q - P^*)$
  - 6: Repeat 2-5 until convergence
  - 7: Project back to the permutation matrix using Hungarian algorithm.
- 

In Fig. 4 we present some illustrations of these algorithms, when using node attributes also. In this example, we use the planar coordinates of nodes of letter graphs as the attributes and incorporate this additional information in matching graphs. The first row is the case without using any node attributes, i.e.  $\lambda = 0$  (in Eqn. 8). In second row, we add node attributes with  $\lambda = 0.5$ . Compared to the first row, this case shows a better

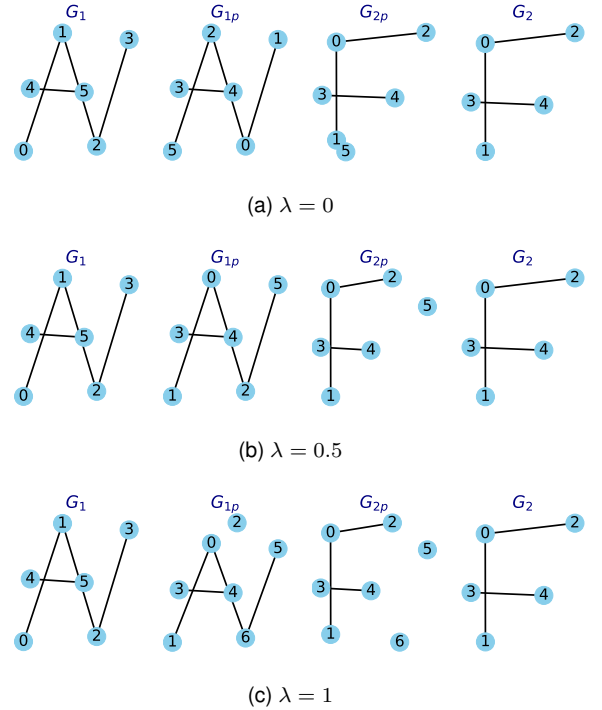


Fig. 4. Example of graph matching using both edge weight and node attributes with different  $\lambda$ . In each row, the outermost graphs, labeled  $G_1$  and  $G_2$ , are the original graphs. The inner two,  $G_{1p}$  and  $G_{2p}$ , are outcomes that are matched to each other. The outcome graphs may have some null nodes added, and the indices of  $G_1$  are permuted as  $G_{1p}$ .

correspondence across graphs since the edges  $0-1$  are now registered across graphs. If we further increase the weight on the node attributes, as last row ( $\lambda = 1$ ) shows, the matching completely ignores the edge correspondence. In second row only one edge  $2-5$  of  $G_{1p}$  is matched to a null edge, while in last row two edges:  $0-6$  and  $5-6$  of  $G_{1p}$  are matched with null edges.

As mentioned earlier, an important strength of this framework is that it provides geodesic paths between registered graphs, as element of the quotient space  $\mathcal{G}$ . The geodesics in the pre-space  $\mathcal{A}$  and the graph space  $\mathcal{G}$  are linear interpolations, except that the registration has been optimized in the latter case. Fig. 5 is a comparison between geodesics in  $\mathcal{A}$  (top row) and in  $\mathcal{G}$  (bottom row) between the same two graphs. The two original graphs are at the two ends, representing letter 'A' and letter 'F'. In this example, we also use the coordinates of nodes as node attributes with  $\lambda = 1$ . As one can see, geodesic in  $\mathcal{G}$  shows a more natural *deformation* from one graph to the other, resulting from an improved matching of nodes.

As stated in the previous section, we can also use Laplacian matrices to represent graphs. Although one can easily map an adjacency matrix to a Laplacian matrix using  $\phi$ , and vice-versa, the past literature has rarely used Laplacian matrix for graph matching. We present one example in Fig. 6 where we perform matching under both the representations – adjacency matrix and Laplacian matrix, using Algorithm 1. As commented earlier, the mapping  $\phi$  is not an isometry  $\|P A_1 P^T - A_2\|^2$  results in a different solutions than mini-

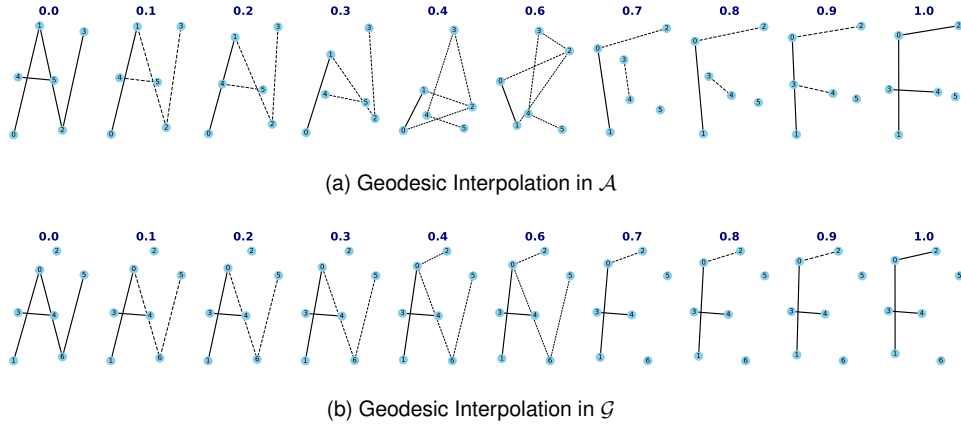


Fig. 5. Comparison between geodesics in original space and graph space for two different graphs,  $\lambda = 1$ . Time point is labeled on the top of each graph while 0 and 1 indicate the original graphs. Dash lines imply that the edges are changing.

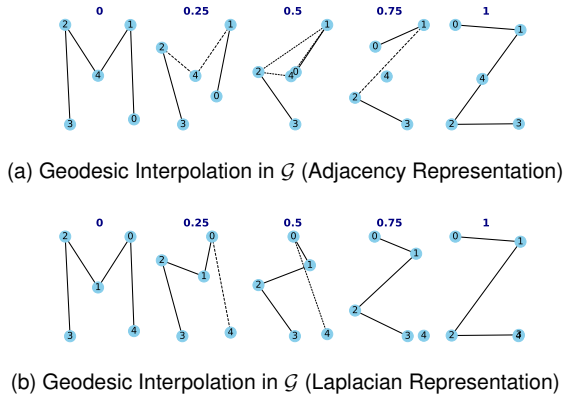


Fig. 6. Comparison between geodesics in graph space using adjacency and Laplacian matrix representation,  $\lambda = 0$ . Time point is labeled on the top of each graph while 0 and 1 indicate the original graphs. Dash lines imply that the edges are changing.

mizing  $\|PL_1P^T - L_2\|^2$ . Anyway, one should note that the different representations of graphs only diverge in terms of actual solutions, the general procedures are quite similar.

## V. STATISTICAL ANALYSIS OF GRAPHS

We have developed a metric space  $\mathcal{G}$  for representing, matching and comparing graphs. Additionally, we have now a way of computing geodesic paths in  $\mathcal{G}$  between arbitrary graphs. Together, these tools help us derive statistical summaries of graph data and develop stochastic models to capture the observed variability in given data. We start by defining simple means and covariances.

### A. Mean of Graph Data

Given a set of graphical data, it is important to summarize given graphs using the notion of a mean or a median. However, a simple average of the adjacency matrices does not make much sense if the nodes are not registered, which is usually the case in practice. Therefore, we would like to seek the mean in the graph space  $\mathcal{G}$ . Given a set of  $m$  graphs,  $G_i \in \mathcal{G}$ ,  $i =$

$1, \dots, m$ , with corresponding adjacency matrices  $A_i \in \mathbb{R}^{n \times n}$ , the adjacency matrix of the mean graph is defined as:

$$A_\mu = \operatorname{argmin}_{A \in \mathbb{R}^{n \times n}} \sum_{i=1}^m d([A], [A_i])^2, \quad (11)$$

where  $d([A], [A_i])$  is as defined in Eqn. 4. An algorithm for computing this mean is given next.

---

### Algorithm 3 Graph Mean in $\mathcal{G}$

---

Given graphs  $G_i$  and the associated adjacency matrix  $A_i$ ,  $i = 1, \dots, m$ :

- 1: Initialize a mean template  $A_\mu$ .
  - 2: Match  $A_i$  to  $A_\mu$  using Algorithm 1 or 2 and store the matched graph as  $A_i^*$ , for  $i = 1, \dots, m$ .
  - 3: Update  $A_\mu = \frac{1}{m} \sum_{i=1}^m A_i^*$ . In case we include node attributes in the analysis, we also perform an averaging of the registered nodes, as discussed below.
  - 4: Repeat 2 and 3 until convergence.
- 

In case the node attributes are included, one will need to endow the node attribute space  $\mathcal{N}$  with a metric structure, so that one can average the nodes also. For Euclidean attributes that is straightforward. However, in case of categorical node attributes, one either needs to impose a metric structure and use that structure to compute the mean node value.

### B. Principal Component Analysis of Graphs

The high dimensionality of observed graphs is a big issue in many problem domains. For a graph with  $n$  nodes, the number of potential edges can be as high as  $\binom{n}{2}$ . It will be useful to have a technique for projecting graph data to smaller dimensions while capturing as much intrinsic variability in the data as possible. Principal component analysis (PCA) can naturally be used as a simple tool for linear projection and dimension reduction, and to discover dominant directions/subspaces in data space. As mentioned earlier, the non-registration of nodes in the raw data can be an obstacle in applying PCA direction in  $\mathcal{A}$ . Instead, one can apply PCA in the quotient space  $\mathcal{G}$  listed in Algorithm 4. After PCA, graphs can be represented as low dimensional vectors, which facilitates further analysis.

Compared with the graph embedding techniques that also represent graphs as vectors [42], one is able to project the principal scores back to the graphs.

Given a set of graphs with adjacency matrices  $A_i \in \mathcal{A}$ , let  $[A_\mu]$  denote their sample mean in  $\mathcal{G}$  (obtained using Algorithm 3) and  $A_i^*$  be the matrices registered to  $A_\mu$ . Then, the differences  $\{A_i^* - A_\mu\}$  are elements of a vector space  $\mathcal{A}$  and one can use them to perform PCA. The algorithm for PCA follows.

---

**Algorithm 4** Graph PCA
 

---

Given graphs  $G_i$  and the associated adjacency matrix  $A_i$ ,  $i = 1, \dots, m$ :

- 1: Find the mean  $A_\mu$  using Algorithm 3 and find the matched graph  $A_i^*$ ,  $i = 1, 2, \dots, m$ .
  - 2: Vectorize  $A_i^* - A_\mu$  and perform PCA. Obtain directions and singular values for the principal components.
- 

As mentioned before, the extended adjacency matrices can be used for the graphs with different number of nodes. In fact, one can also elongate  $\{A_i^* - A_\mu\}$  with node attributes when nodes are taken into account. We skip further discussions on these possibilities to save space.

### C. Generative Graph Model

In some situations involving statistical inferences, it is useful to develop analytical generative models for graphical data. For example, it can be useful in performing Bayesian graphical inference [43]. However, model estimation directly from observed graphs may have a large error because the graphs are not registered. We introduce a simple Gaussian-type model in graph space  $\mathcal{G}$  to better capture the essential variability of graphical data. In conjunction with the graph PCA and potential dimension reduction, we can reach a very efficient model.

Assume that we have a set of graphs with adjacency matrices  $A_i$ ,  $i = 1, \dots, m$ . By applying Algorithm 4, we can get the PC scores  $s_i \in \mathbb{R}^k$  by projecting each  $A_i$  to the first  $k$  principal components space. For  $s_i$ s, we impose a  $k$  dimensional Gaussian model with sample mean and covariance as the model parameters. Note that Gaussian model is used only for illustration, but any general parametric or nonparametric model can also be used here. In case one wants to use a multivariate normal density, it is useful to validate it using some normality test beforehand. Unlike the generative graph model in [44], where one need to gradually add nodes and edges to get a new sample graph. One can directly sample a new graph from the proposed model.

## VI. EXPERIMENTS AND APPLICATIONS

To illustrate this framework, we have implemented it on a variety of graph datasets. The results are presented in this section.

### A. Letter Shapes

The Letter Graphs dataset is a part of the IAM Graph Database used in [37], and consist of small graphs depicting

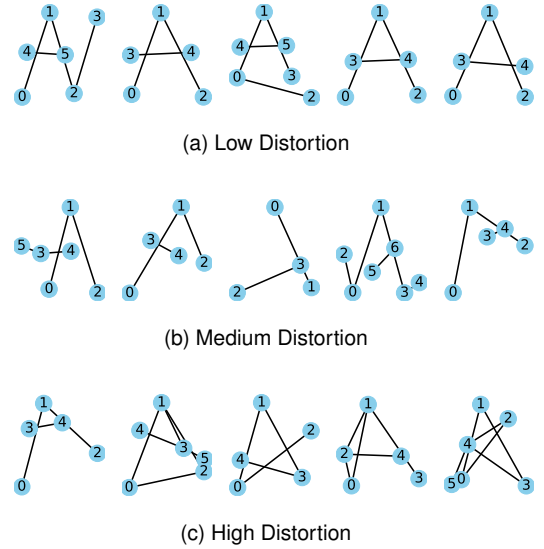


Fig. 7. Sample graphs of Letter 'A' in different levels of distortion

15 uppercase letters (A, E, F, H, I, K, L, M, N, T, V, W, X, Y, Z) that can be drawn using straight lines. The edge weights in these graphs are either one or zero. The nodes have location coordinates in  $\mathbb{R}^2$  so that the collection of edges form the shape of a letter. The authors also introduced distortions to the prototype graphs with three different levels of distortions – low, medium and high. Fig. 7 shows some sample graphs of letter 'A' at these three different distortion levels.

First, we use Algorithm 3 to compute mean graphs of 50 observations associated with letter 'A', at each of the three distortion levels. The results are shown in Fig. 8. In order to match different number of nodes across multiple graphs, one has to add a number of null nodes in the mean shape, and this can be seen in the resulting means. The mean graphs resemble the letter 'A' in all three cases, despite a significant variability and distortions in the original data.

Additionally, we perform PCA on this letter data in the quotient space  $\mathcal{G}$  and display results in Figs. 9, 10 and 11, for low, medium and high distortion graphs, respectively. In these figures, each row depicts shape variability along a principal direction in the given data in form of graphs at mean  $0, \pm 1, \pm 2$  standard deviation. This analysis helps identify the main modes of structural variability in the original data. For example, Fig. 9 shows graphs along first three principal directions of variability in the *low distortion* dataset. In all these graphs, the main edges are stable and there are no significant changes along principal axes. This implies that observations in this set are quite similar in shape. However, in results from the medium distortion data in Fig. 10, the horizontal edge  $3 - 4$  changes significantly in the first principal direction. In case of the high distortion level, there are significant changes in shapes along principal directions. For instance, in the top row, there is an extra edge  $1 - 4$  on the top left that dominates the first principal direction.

Another important application of PCA is in reducing data dimension. That is, perform PCA on graph data and represent original graphs using low-dimensional PC scores. One can



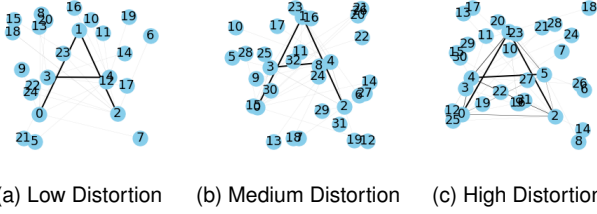


Fig. 8. Mean graphs of letter 'A'

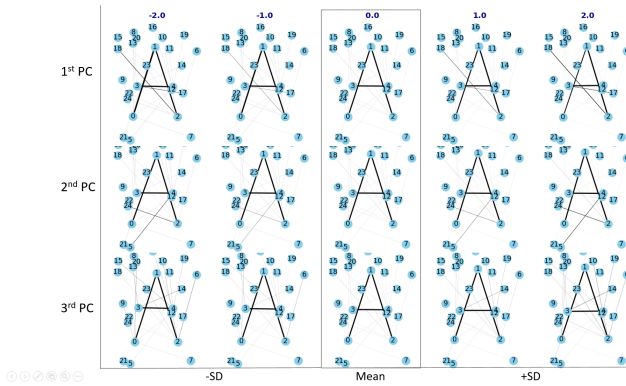


Fig. 9. First three principal variations of letter 'A', low distortion. From top to bottom, each row shows the variation for the first, second and third principal directions, respectively. For each row, the middle one is mean while toward left and right, they are the graphs after perturbing the mean by one and two square root of singular value.

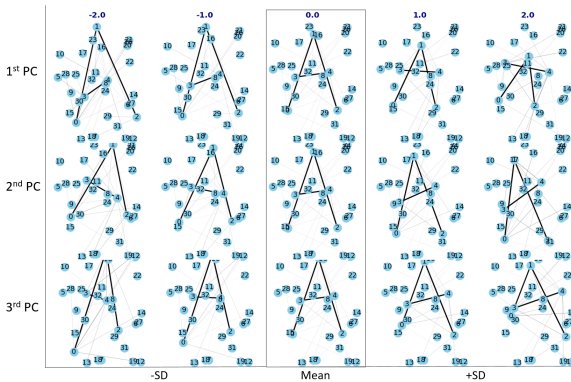


Fig. 10. First three principal variations of letter 'A', medium distortion. From top to bottom, each row shows the variation for the first, second and third principal directions, respectively. For each row, the middle one is mean while toward left and right, they are the graphs after perturbing the mean by one and two square root of singular value.

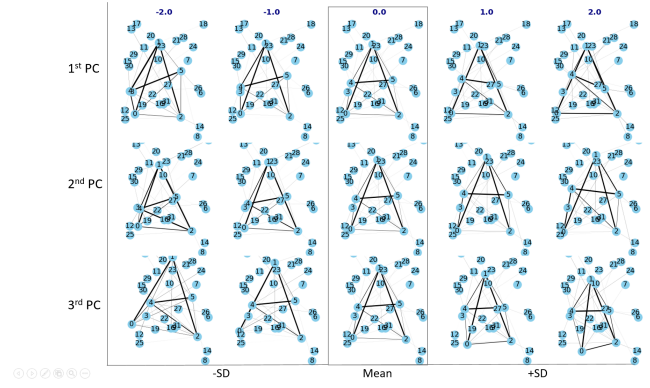


Fig. 11. First three principal variations of letter 'A', high distortion. From top to bottom, each row shows the variation for the first, second and third principal directions, respectively. For each row, the middle one is mean while toward left and right, they are the graphs after perturbing the mean by one and two square root of singular value.

	> 70%	> 80%	> 90%	100%
Low	13	16	18	50
Medium	11	16	25	50
High	11	14	21	50

TABLE I  
LETTER A: NUMBER OF PCs NEEDED FOR INDICATED VARIANCE

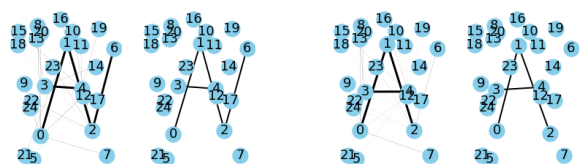
reconstruct and visualize these approximate graphs, to evaluate the quality of representation. Fig. 12 shows the reconstruction of graphs using only the first 16, 16 and 14 dimensions for low, medium and high distortion letters, respectively. These dimensions were chosen to ensure the representation retains at least 80% of the original variance. The reconstructed graphs are quite similar to the original despite a significant reduction in size. Fig. 13 shows percentage variance in first  $d$  components versus  $d$ , while the actual cutoffs can be found in Table I.

Additionally, we fitted a Gaussian model on PC scores of the observed graphs. We first use PCA to reduce the dimension to around 80% variance as mentioned before. Then we impose a Gaussian model on these principal component scores. To test model performance, we generate some random samples from this model and project into graph space, presented in Fig. 14. A visible similarity of these random samples to the original graphs underscores the goodness of the model.

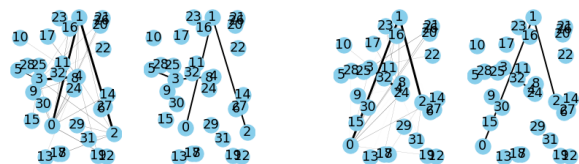
As the final experiment with letters, we perform the following classification experiment. The full letter dataset consists of training, validation and test subsets, each containing 750 graphs. The graphs are uniformly distributed over different letters, i.e., 50 graphs for each class. We classify the graphs based on their pairwise distance in graph space using Algorithm 1. We use Support Vector Machine (SVM) with the radial kernel as the classifier and the classification result on the test data is given in Table III with the comparison from [37].

### B. Molecular Shapes

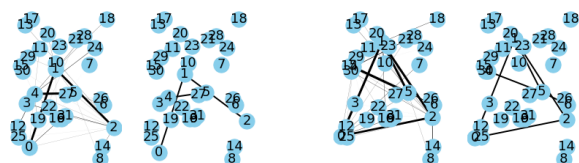
In this section, we analyze another graph dataset from IAM Graph Database [37] that involves shapes of molecular compounds. These molecules are converted into graphs in a



(a) Low Distortion

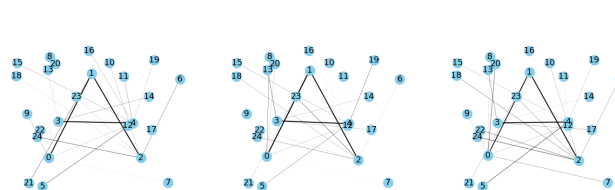


(b) Medium Distortion

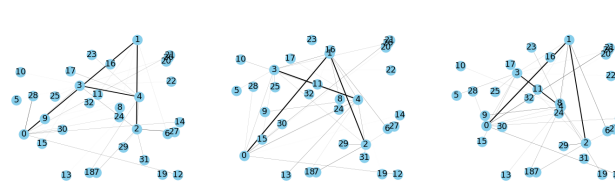


(c) High Distortion

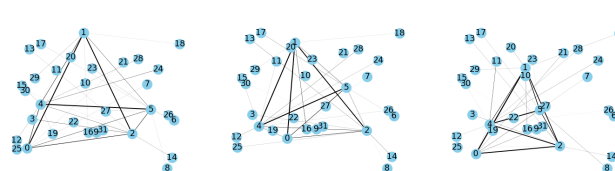
Fig. 12. Reconstructed graphs of letter 'A' using 80% of variations. For each pair, left is the reconstruction while right is the original matched graph.



(a) Low Distortion

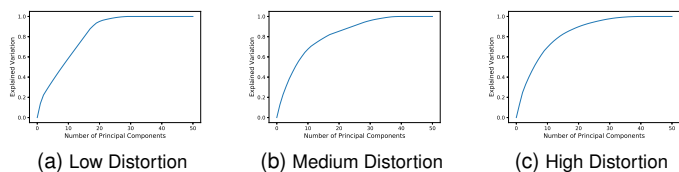


(b) Medium Distortion



(c) High Distortion

Fig. 14. Random samples of letter 'A' from Gaussian model, for the three letter A datasets.



(a) Low Distortion

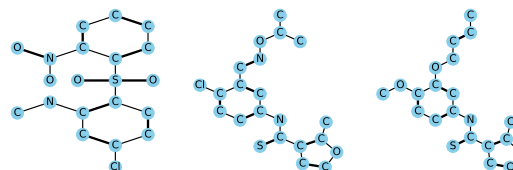
(b) Medium Distortion

(c) High Distortion

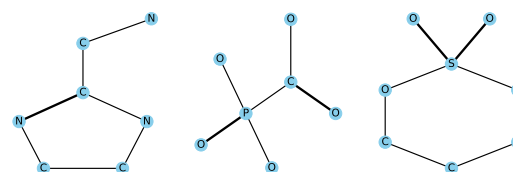
Fig. 13. Cumulative explained variation of letter 'A' by PCA. Vertical axis is the percentage of explained variation while horizontal axis is the number of principal components.

straightforward manner by representing atoms as nodes and the covalent bonds as edges. That is, edges are weighted by valence and node is attributed as atoms. This dataset consists of two classes (active, inactive), which represent molecules with activity against HIV or not. Fig. 15 shows some example graphs of active and inactive molecules. We use the edge weight for matching the graphs and we present one pair of geodesics in  $\mathcal{A}$  and  $\mathcal{G}$  in Fig. 16. The deformation in graph space has more natural path.

The complex structure of molecules results in the high-dimensional representation in the graph space  $\mathcal{G}$ , but that can be handled by PCA. We use the first 22 and 21 principal components for active and inactive classes, respectively, containing roughly 80% of the total variance, to represent and reconstruct these molecules. As shown in Fig. 17, one can successfully reconstruct the original graphs with the chosen smaller dimensions. Fig. 18 shows the percentage variance in top components, versus the number of principal components. The detailed cutoff values can be found in Table II.



(a) Active



(b) Inactive

Fig. 15. Sample graphs of molecules.

	> 70%	> 80%	> 90%	100%
Active	16	22	31	50
Inactive	15	21	31	190

TABLE II  
EXPLAINED PERCENTAGE BY NUMBER OF PRINCIPAL VARIATION FOR MOLECULE GRAPHS

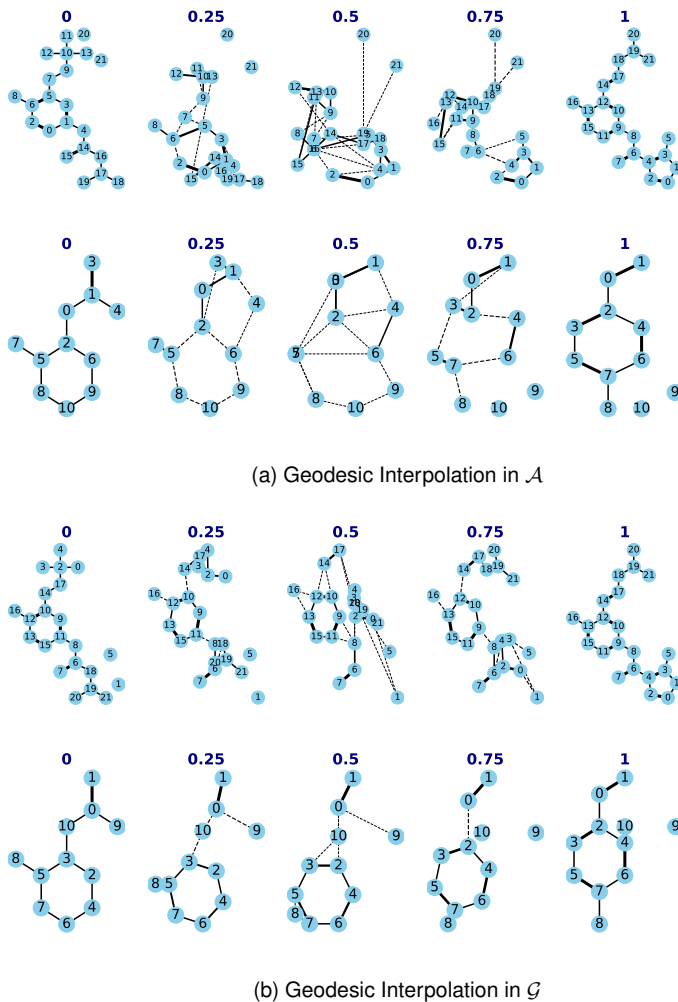


Fig. 16. Comparison between geodesics in original space and graph space for two different molecule graphs in the same class. In each subplot, top is for active molecules while bottom is for inactive molecules. Time point is labeled on the top of each graph while 0 and 1 indicate the original graphs. Dash lines imply that the edges are changing.

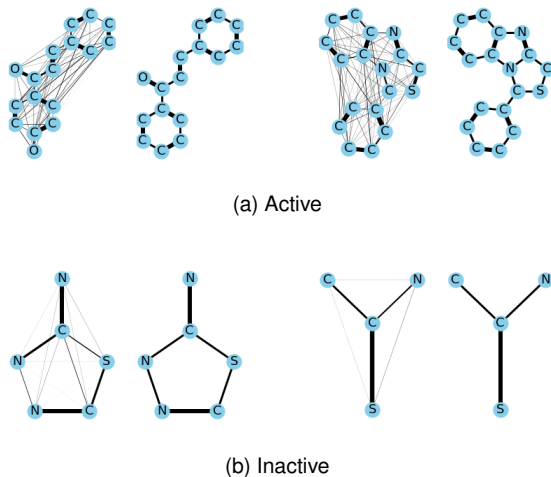


Fig. 17. Reconstructed graphs of molecules. For each pair, left is the reconstruction while right is the original graph. Some null nodes have been removed for a better display.

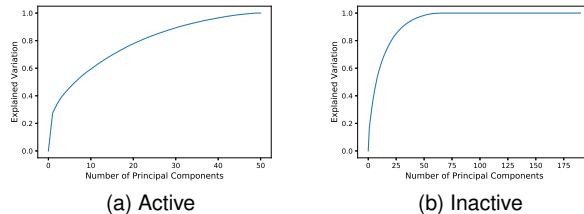


Fig. 18. Cumulative explained variation of molecules by PCA. Vertical axis is the percentage of explained variation while horizontal axis is the number of principal components.

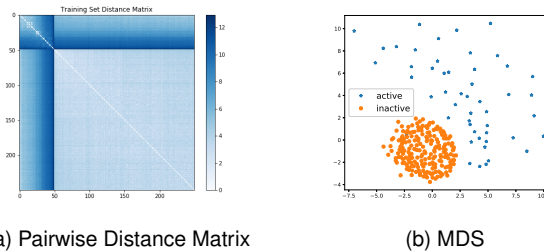


Fig. 19. Pairwise distance matrix and MDS plot of molecule graphs. For distance matrix, first 50 instances are active while the remaining 200 are inactive. For MDS plot, blue star represent active molecules while red dot represent inactive molecules.

This dataset consists of a training set and a validation set of size 250 each, and a test set of size 1,500. Thus, there are 2,000 elements totally. Of those, 1,600 inactive elements and 400 active elements are uniformly distributed over different datasets. We perform classification on this dataset using SVM classifier and the pairwise graph distance (Fig. 19) in  $\mathcal{G}$ . To involve node attributes (atoms values) in the analysis, we adopt a binary distance for nodes. In other words, if two nodes have exactly the same atom, then the distance between them is set to zero. Otherwise it is set to one. In this experiment, we use  $\lambda = 1$  in Eqn. 8 to balance the edge information with node attributes. The classification result on the test data is given in Table III. The results are compared to those presented in the original paper [37].

### C. Video Graphs

The third example comes from representation of cooking videos as pattern theoretic graphs, as developed in [45]. There are 1020 graphs representing 102 different video clips related to cooking. Specifically, for each video clip there are 10 graphs providing multiple interpretations of that video clip [45]. The nodes in a graph represent features extracted from the video and edges represent their interactions or relationships. For

Methods	Letter: Low Distortion	Letter: Medium Distortion	Letter: High Distortion	Molecule
Algorithm 1	98.5%	96.4%	93.6%	99.6%
[37]	99.6%	94.0%	90.0%	97.3%

TABLE III  
CLASSIFICATION RESULT

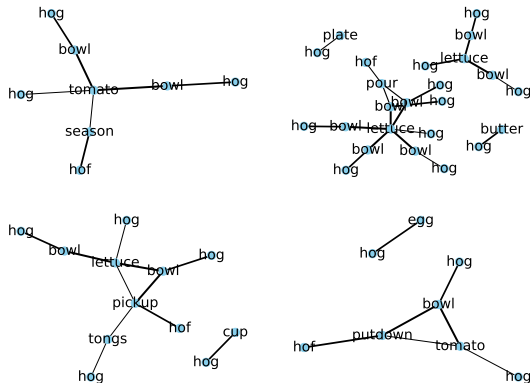


Fig. 20. Sample videos graphs

Edge (E) Only	E + Node-Level $\lambda = 1$	E + Node-Level $\lambda = 2$	E + Node-Name $\lambda = 1$
71.3%	72.3%	73.0%	73.2%

TABLE IV  
VIDEO GRAPHS CLASSIFICATION RESULT

example, a node at the lowest level can be histogram of oriented gradients (HOG) or histogram of optic flow (HOF) features. At the second level, a node can be an object such as a bowl, cup, etc, and at the highest level a node can be an action such as stir, pour, etc. The weight of edges represents the strength of the interaction between the nodes. Some examples of such graphs can be found in Fig. 20.

We will represent each video clip as a different class, and will classify videos using their graphical representations. We perform this classification task using the Nearest Neighbors classifier under the pairwise graph distance in  $\mathcal{G}$ . To utilize node attributes, we also impose a binary distance on node level or node name with different weight. The leave one out result of classification can be found in Table IV.

#### D. Wikipedia Graphs

Our last example comes from communication networks of the Chinese Wikipedia [46], [47]. In these graphs, nodes represent users of the Chinese Wikipedia, and an edge (0 or 1) denotes whether one user left a message on the talk page to another user at a certain time stamp. We take monthly graphs from the year 2004, resulting in a sample size of 12 graphs. On average, each graph has around 300 nodes and 431 edges. We compute the mean in original space  $\mathcal{A}$  and graph space  $\mathcal{G}$ , with results shown in Fig. 21. The top panel is simply an average of adjacency matrix. It is complex and hard to discern any pattern from this average. The bottom panel shows the mean in graph space; this graph shows a clear clustering of users implying that there are prominent subsets of users that actively interact with others in their clusters.

The results from PCA analysis of these graphs is shown in Fig. 22. These results show that most of the user interactions

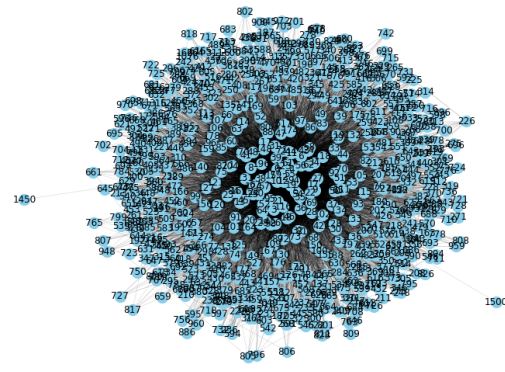
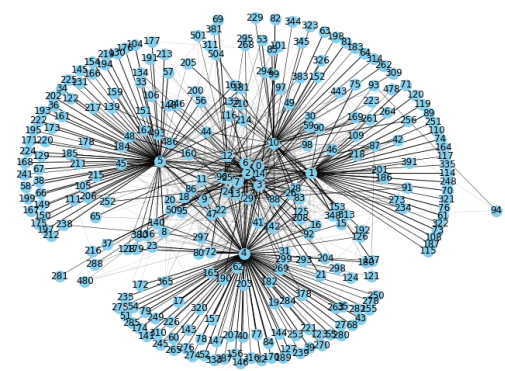
(a) Mean in  $\mathcal{A}$ (b) Mean in  $\mathcal{G}$ 

Fig. 21. Comparison of means in different space for Wikipedia graphs.

are stable and remain unchanged, while principal variations in the data come only from a handful of active users.

## VII. DISCUSSION & CONCLUSION

In this paper, we presented a novel framework for learning and analyzing structures of graphs. The quotient space formulation removes the nuance permutation variability. Due to the isometric action of the permutation group, the quotient space inherits metric that enables metric-based statistical analysis of graphs – geodesics, means, PCA, and Gaussian-type models.

The set of tools developed in this paper are useful in several contexts. For instance, one can use them to analyze methods in geometrical deep learning, where both data and inferences can involve graphs in different forms. Low-dimensional Euclidean representations of graphs will enable a direct use of more sophisticated statistical models, including many deep learning architectures. The ability to reconstruct full graphs from these representations is important in synthesizing new graphs.

One limitation of the current formulation is that the edge attribute is restricted to be Euclidean ( $M = \mathbb{R}$ ). However, the

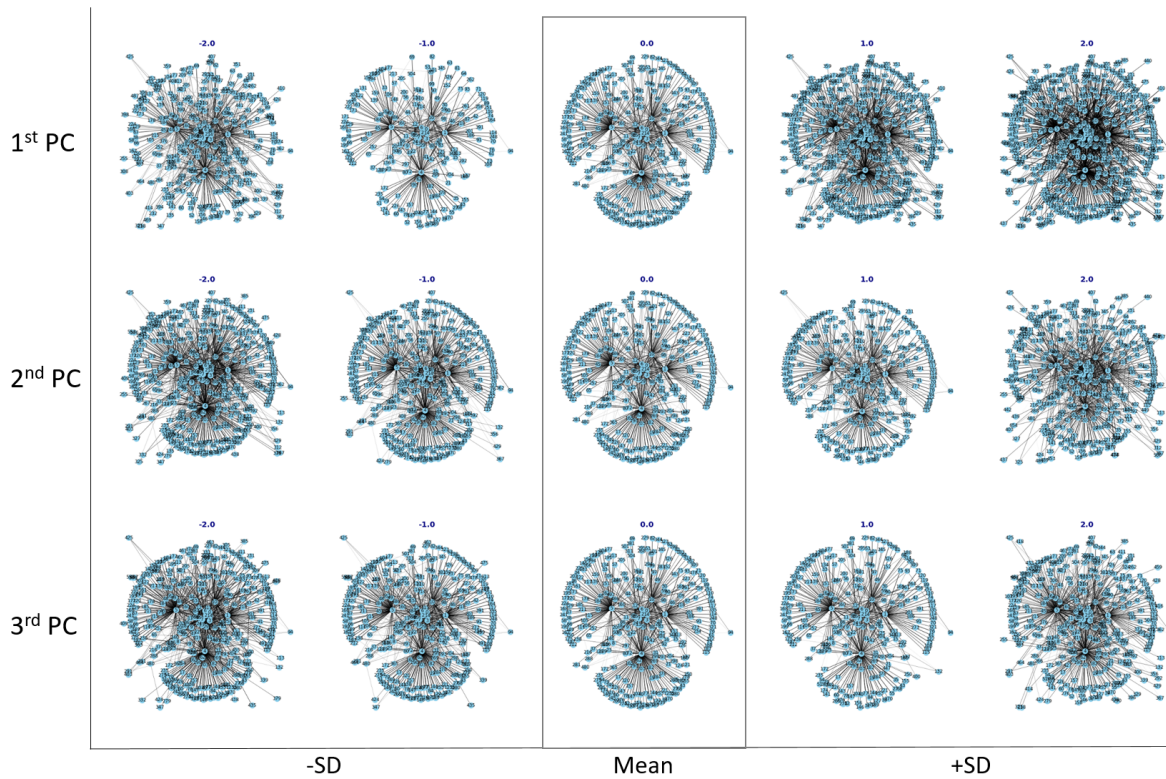


Fig. 22. First 3 principal variations of Wikipedia graphs. From top to bottom, each row shows the variation for the first, second and third principal directions, respectively. For each row, the middle one is mean while toward left and right, they are the graphs after perturbing the mean by one and two square root of singular value.

future work includes investigating the applications of cases when graphs have more generic edge attributes.

#### ACKNOWLEDGMENT

The authors would like to thank the creators of different public datasets used in this paper. The authors also thank Dr. Adam Duncan for his contributions in the implementation of a preliminary version of the approach.

#### REFERENCES

- [1] F. D. De Souza, S. Sarkar, A. Srivastava, and J. Su, "Pattern theory-based interpretation of activities," in *Pattern Recognition (ICPR), 2014 22nd International Conference on*. IEEE, 2014, pp. 106–111.
- [2] J. Ugander, B. Karrer, L. Backstrom, and C. Marlow, "The anatomy of the facebook social graph," *arXiv preprint arXiv:1111.4503*, 2011.
- [3] M. A. Westenberg, S. A. van Hijum, A. T. Lulko, O. P. Kuipers, and J. B. Roerdink, "Interactive visualization of gene regulatory networks with associated gene expression time series data," in *Visualization in Medicine and Life Sciences*. Springer, 2008, pp. 293–311.
- [4] M. Dai, Z. Zhang, and A. Srivastava, "Testing stationarity of brain functional connectivity using change-point detection in fmri data," in *Proceedings of the IEEE Conference on Computer Vision and Pattern Recognition Workshops*, 2016, pp. 19–27.
- [5] W. A. Mackaness and K. M. Beard, "Use of graph theory to support map generalization," *Cartography and Geographic Information Systems*, vol. 20, no. 4, pp. 210–221, 1993.
- [6] J. Yang, "Market segmentation and information asymmetry in chinese stock markets: A var analysis," *Financial Review*, vol. 38, no. 4, pp. 591–609, 2003.
- [7] S. L. Hakimi, "Optimum distribution of switching centers in a communication network and some related graph theoretic problems," *Operations research*, vol. 13, no. 3, pp. 462–475, 1965.
- [8] M. D. Shirley and S. P. Rushton, "The impacts of network topology on disease spread," *Ecological Complexity*, vol. 2, no. 3, pp. 287–299, 2005.
- [9] D. C. Van Essen, S. M. Smith, D. M. Barch, T. E. Behrens, E. Yacoub, K. Ugurbil, W.-M. H. Consortium *et al.*, "The wu-minn human connectome project: an overview," *Neuroimage*, vol. 80, pp. 62–79, 2013.
- [10] A. Narayanan, M. Chandramohan, R. Venkatesan, L. Chen, Y. Liu, and S. Jaiswal, "graph2vec: Learning distributed representations of graphs," *arXiv preprint arXiv:1707.05005*, 2017.
- [11] Y. Bai, H. Ding, Y. Qiao, A. Marinovic, K. Gu, T. Chen, Y. Sun, and W. Wang, "Unsupervised inductive graph-level representation learning via graph-graph proximity," in *IJCAI*, 2019.
- [12] B. Perozzi, R. Al-Rfou, and S. Skiena, "Deepwalk: Online learning of social representations," in *Proceedings of the 20th ACM SIGKDD international conference on Knowledge discovery and data mining*. ACM, 2014, pp. 701–710.
- [13] A. Grover and J. Leskovec, "node2vec: Scalable feature learning for networks," in *Proceedings of the 22nd ACM SIGKDD international conference on Knowledge discovery and data mining*. ACM, 2016, pp. 855–864.
- [14] D. Wang, P. Cui, and W. Zhu, "Structural deep network embedding," in *Proceedings of the 22nd ACM SIGKDD international conference on Knowledge discovery and data mining*. ACM, 2016, pp. 1225–1234.
- [15] J. Tang, M. Qu, M. Wang, M. Zhang, J. Yan, and Q. Mei, "Line: Large-scale information network embedding," in *Proceedings of the 24th international conference on world wide web*. International World Wide Web Conferences Steering Committee, 2015, pp. 1067–1077.
- [16] H. Chen, B. Perozzi, Y. Hu, and S. Skiena, "Harp: Hierarchical representation learning for networks," in *Thirty-Second AAAI Conference on Artificial Intelligence*, 2018.
- [17] A. Ortega, P. Frossard, J. Kovačević, J. M. Moura, and P. Vandergheynst, "Graph signal processing: Overview, challenges, and applications," *Proceedings of the IEEE*, vol. 106, no. 5, pp. 808–828, 2018.
- [18] M. Defferrard, X. Bresson, and P. Vandergheynst, "Convolutional neural networks on graphs with fast localized spectral filtering," in *Advances in neural information processing systems*, 2016, pp. 3844–3852.

- [19] T. N. Kipf and M. Welling, "Semi-supervised classification with graph convolutional networks," *arXiv preprint arXiv:1609.02907*, 2016.
- [20] W. Hamilton, Z. Ying, and J. Leskovec, "Inductive representation learning on large graphs," in *Advances in Neural Information Processing Systems*, 2017, pp. 1024–1034.
- [21] M. Neuhaus and H. Bunke, *Bridging the gap between graph edit distance and kernel machines*. World Scientific, 2007, vol. 68.
- [22] V. Carletti, P. Foggia, A. Saggese, and M. Vento, "Challenging the time complexity of exact subgraph isomorphism for huge and dense graphs with vf3," *IEEE transactions on pattern analysis and machine intelligence*, vol. 40, no. 4, pp. 804–818, 2017.
- [23] F. Zhou and F. De la Torre, "Factorized graph matching," in *Computer Vision and Pattern Recognition (CVPR), 2012 IEEE Conference on*. IEEE, 2012, pp. 127–134.
- [24] D. Conte, P. Foggia, C. Sansone, and M. Vento, "Thirty years of graph matching in pattern recognition," *International journal of pattern recognition and artificial intelligence*, vol. 18, no. 03, pp. 265–298, 2004.
- [25] S. Umeyama, "An eigendecomposition approach to weighted graph matching problems," *IEEE transactions on pattern analysis and machine intelligence*, vol. 10, no. 5, pp. 695–703, 1988.
- [26] T. Caelli and S. Kosinov, "An eigenspace projection clustering method for inexact graph matching," *IEEE transactions on pattern analysis and machine intelligence*, vol. 26, no. 4, pp. 515–519, 2004.
- [27] S. Gold and A. Rangarajan, "A graduated assignment algorithm for graph matching," *IEEE Transactions on pattern analysis and machine intelligence*, vol. 18, no. 4, pp. 377–388, 1996.
- [28] V. Lyzinski, D. E. Fishkind, M. Fiori, J. T. Vogelstein, C. E. Priebe, and G. Sapiro, "Graph matching: Relax at your own risk," *IEEE transactions on pattern analysis and machine intelligence*, vol. 38, no. 1, pp. 60–73, 2016.
- [29] K. Riesen and H. Bunke, "Approximate graph edit distance computation by means of bipartite graph matching," *Image and Vision computing*, vol. 27, no. 7, pp. 950–959, 2009.
- [30] H. Almohamad and S. O. Duffuaa, "A linear programming approach for the weighted graph matching problem," *IEEE Transactions on pattern analysis and machine intelligence*, vol. 15, no. 5, pp. 522–525, 1993.
- [31] M. Krčmar and A. Dhawan, "Application of genetic algorithms in graph matching," in *Proceedings of 1994 IEEE International Conference on Neural Networks (ICNN'94)*, vol. 6. IEEE, 1994, pp. 3872–3876.
- [32] P. E. Hart, N. J. Nilsson, and B. Raphael, "A formal basis for the heuristic determination of minimum cost paths," *IEEE transactions on Systems Science and Cybernetics*, vol. 4, no. 2, pp. 100–107, 1968.
- [33] B. J. Jain and K. Obermayer, "Structure spaces," *Journal of Machine Learning Research*, vol. 10, no. Nov, pp. 2667–2714, 2009.
- [34] —, "Learning in riemannian orbifolds," *arXiv preprint arXiv:1204.4294*, 2012.
- [35] R. Horaud, "A short tutorial on graph laplacians, laplacian embedding, and spectral clustering."
- [36] K. Severn, I. L. Dryden, and S. P. Preston, "Manifold valued data analysis of samples of networks, with applications in corpus linguistics," *arXiv preprint arXiv:1902.08290*, 2019.
- [37] K. Riesen and H. Bunke, "Iam graph database repository for graph based pattern recognition and machine learning," in *Joint IAPR International Workshops on Statistical Techniques in Pattern Recognition (SPR) and Structural and Syntactic Pattern Recognition (SSPR)*. Springer, 2008, pp. 287–297.
- [38] J. T. Vogelstein, J. M. Conroy, V. Lyzinski, L. J. Podrazik, S. G. Kratzer, E. T. Harley, D. E. Fishkind, R. J. Vogelstein, and C. E. Priebe, "Fast approximate quadratic programming for graph matching," *PLOS one*, vol. 10, no. 4, p. e0121002, 2015.
- [39] M. Frank and P. Wolfe, "An algorithm for quadratic programming," *Naval research logistics quarterly*, vol. 3, no. 1-2, pp. 95–110, 1956.
- [40] W. contributors, "Erdsrnyi model — Wikipedia, the free encyclopedia," 2018, [Online; accessed 22-February-2019]. [Online]. Available: [https://en.wikipedia.org/w/index.php?title=Erdsrnyi\\_model&oldid=849961686](https://en.wikipedia.org/w/index.php?title=Erdsrnyi_model&oldid=849961686)
- [41] H. W. Kuhn, "The hungarian method for the assignment problem," *Naval research logistics quarterly*, vol. 2, no. 1-2, pp. 83–97, 1955.
- [42] H. Bahonar, A. Mirzaei, S. Sadri, and R. Wilson, "Graph embedding using frequency filtering," *IEEE transactions on pattern analysis and machine intelligence*, 2019.
- [43] F. V. Jensen *et al.*, *An introduction to Bayesian networks*. UCL press London, 1996, vol. 210.
- [44] L. Han, R. C. Wilson, and E. R. Hancock, "Generative graph prototypes from information theory," *IEEE transactions on pattern analysis and machine intelligence*, vol. 37, no. 10, pp. 2013–2027, 2015.
- [45] F. Souza, S. Sarkar, A. Srivastava, and J. Su, "Temporally coherent interpretations for long videos using pattern theory," in *Proceedings of the IEEE Conference on Computer Vision and Pattern Recognition*, 2015, pp. 1229–1237.
- [46] "Wikipedia talk, chinese network dataset – KONECT," Apr. 2017. [Online]. Available: [http://konect.uni-koblenz.de/networks/wiki\\_talk\\_zh](http://konect.uni-koblenz.de/networks/wiki_talk_zh)
- [47] J. Sun, J. Kunegis, and S. Staab, "Predicting user roles in social networks using transfer learning with feature transformation," in *Proc. ICDM Workshop on Data Mining in Networks*, 2016.